Ludden, J.N., Plank, T., and Escutia, C. (Eds.)
Proceedings of the Ocean Drilling Program, Scientific Results Volume 185

6. Cretaceous Radiolarian Biochronology and Carbon Isotope Stratigraphy of ODP Site 1149 (Northwestern Pacific, Nadezhda Basin)[1]

Annachiara Bartolini[2]

ABSTRACT

In the Nadezhda Basin (northwestern Pacific), the contact between oceanic crust basalt and its sedimentary cover was recovered at Site 1149 during Leg 185. The bottom sedimentary section (Unit IV) is characterized by interbedded radiolarian chert and radiolarian nannofossil chalk/marl. This peculiar lithology for the western Pacific has allowed an approach of integrated stratigraphy between radiolarians and carbon isotope data. The upper Valanginian $\delta^{13}C$ positive excursion, correlatable to magnetic Chron M11, was individuated. Biochemostratigraphy constrains the calibration of the positive magnetic lineation at Site 1149 as Chron M12r. Moreover, these data confirm the upper Valanginian $\delta^{13}C$ positive excursion as a global event, probably linked to high primary productivity.

INTRODUCTION

Site 1149 is located at 31.3°N, 143.3°E, on the Pacific plate in the Nadezhda Basin southeast of Japan, at a water depth of ~5800 m. It resides among low abyssal hills on a slight high ~100 km east of the Izu-Bonin Trench (Fig. F1), where the Pacific plate is flexed upward prior to its entry into the subduction zone. In the Nadezhda Basin, the sediment/

F1. ODP Site 1149, p. 14.

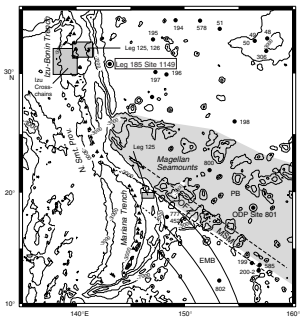

[1]Bartolini, A., 2003. Cretaceous radiolarian biochronology and carbon isotope stratigraphy of ODP Site 1149 (northwestern Pacific, Nadezhda Basin). *In* Ludden, J.N., Plank, T., and Escutia, C. (Eds.), *Proc. ODP, Sci. Results,* 185, 1–17 [Online]. Available from World Wide Web: <http://www-odp.tamu.edu/publications/185_SR/VOLUME/CHAPTERS/011.PDF>. [Cited YYYY-MM-DD]
[2]Laboratoire de Micropaléontologie, case 104, Université Pierre et Marie Curie, 4 Place Jussieu, 75252 Paris 05, France. **chiara@ccr.jussieu.fr**

Initial receipt: 7 November 2001
Acceptance: 27 September 2002
Web publication: 19 February 2003
Ms 185SR-011

basement contact was recovered during Leg 185 in three holes (Holes 1149B, 1149C, and 1149D) and a complete sedimentary section was cored from Lower Cretaceous to Pleistocene in Hole 1149B. Radiolarians were investigated in detail from Units IV and III in Hole 1149B (Fig. F2) and at the sediment/basement contact in all the three holes. Unit IV consists of interbedded radiolarian chert and radiolarian nannofossil chalk/marl. Unit III is characterized by the disappearance of carbonate and by the presence of alternating siliceous lithologies ranging from opal-CT–rich and zeolite-bearing clay to radiolarian porcellanite and radiolarian chert.

Based on its Cretaceous paleolatitude history, Site 1149 may have formed at ~5°S, drifted south to 10°S in its early history, then gradually drifted north, crossing the paleoequator as the Pacific accelerated its northward motion during the Cretaceous (Plank, Ludden, Escutia, et al., 2000). Low-latitude radiolarian assemblages recovered at Site 1149 compare very well with low-latitude Tethyan fauna (e.g., Jud, 1994; O'Dogherty, 1994; Baumgartner et al., 1995a). For this reason, it was possible in this study to use the biozonations of Baumgartner et al. (1995b) and of O'Dogherty (1994) established in low-latitude Tethyan land sections. The advantages of using these biozonations are twofold:

1. These biozonations were established by using the Unitary Associations (UA) method (Guex, 1991), which is helpful in analyzing discontinuous biostratigraphic data such as the ones studied herein.
2. The Early Cretaceous biozonation of Baumgartner et al. (1995b) was correlated directly both with magneto and carbon isotope stratigraphy.

Because of low core recovery, no magnetostratigraphy was possible in Hole 1149B for Units IV and III. For Unit IV, an approach of integrated stratigraphy between carbon stable isotopes and radiolarian Unitary Association Zones (UAZ 95) of Baumgartner et al. (1995b) allows us to better define the age determination and to correlate indirectly with the magnetostratigraphy established in Tethyan land sections (Lini et al., 1992; Channell et al., 1993; Jud, 1994; Baumgartner et al., 1995b). The biochemostratigraphy data presented here provide constraints on the magnetostratigraphic location of basement at Site 1149. Moreover, a relatively continuous Valanginian–Hauterivian $\delta^{13}C$ curve is well documented for the first time in the northwestern Pacific.

F2. Lithostratigraphic section and radiolarian biochronology, Units IV and III, p. 15.

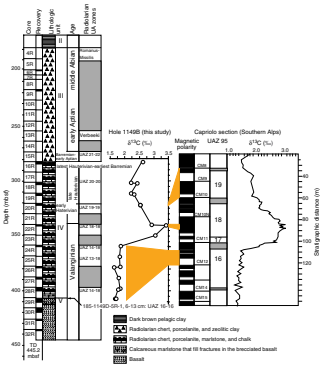

F3. Samples from Unit IV, p. 16.

RADIOLARIAN DATA

Radiolarians were extracted from samples first using HCl to remove the carbonate component and then using diluted HF (1%–5%). Eighteen moderately well preserved samples were selected. All specimens were picked and then observed with scanning electronic microscope. For our purpose, to furnish a chronological framework for the Cretaceous interval of Site 1149, only taxa included in zonations of O'Dogherty (1994) and Baumgartner et al. (1995b) were treated (Fig. F3). The taxonomic identifications (see "Appendix," p. 9) generally follow O'Dogherty (1994) and Baumgartner et al. (1995), with some modifications after Dumitrica and Dumitrica-Jud (1995), Dumitrica et al. (1997), and Dumitrica (1997). To obtain the best possible correlation with the UAZ 95, the radiolarian data set of Unit IV (Fig. F3) were run against the

127 UAs (which form the basis of the UAZ 95 standard) using the computer program BioGraph (Savary and Guex, 1999).

Unit IV

In Hole 1149D, in the sediments just overlying basalts, a well-preserved radiolarian sample (Sample 185-1149D-5R-1, 6–13 cm) was recovered. In this sample, the radiolarian assemblage of *Eucyrtis columbaria* Renz, *Sethocapsa tricornis* Jud, *Cecrops septemporatus* (Parona), and *Parvicingula*? sp. aff. *Parvincingula cincta* (Hinde) sensu Baumgartner et al. (1995a), indicates UAZ 95 16 (Fig. F3). In the Tethyan land section, UAZ 95 16 corresponds to the magnetic polarity Zones M14 to lower M12 normal (lower Valanginian) (Fig. F2) (Jud, 1994; Baumgartner et al., 1995b).

In Holes 1149C and 1149B, sediments immediately overlying basalt contain poorly preserved radiolarian assemblages dominated by long-ranging species.

In Hole 1149B, the lowermost well-preserved sample is Sample 185-1149B-22R-1, 14–19 cm (Fig. F2). The concurrent presence of *Emiluvia chica* Foreman, *Mirifusus petzholdti* (Rüst), *C. septemporatus,* and *Pseudodictyomitra lilyae* (Tan) attributes this sample to UAZ 95 18 (Fig. F3). In the Tethyan land sections (southern Alps and central Apennines in Italy), UAZ 95 18 was correlated with part of M11 and the upper Valanginian $\delta^{13}C$ positive peak (Fig. F2) (Lini et al., 1992; Channell et al., 1993; Jud, 1994; Baumgartner et al., 1995b).

Samples 185-1149B-20R-1, 116–120 cm, and 20R-1, 55–57 cm, are assigned to UAZ 95 19 (Fig. F3), which was correlated to the M10–M9 interval (early Hauterivian) (Fig. F2) (Jud, 1994; Baumgartner et al., 1995b). Sample 185-1149B-20R-1, 116–120 cm, is characterized by the presence of *Crucella lipmanae* Jud and *Spongocapsula*? *tripes* Jud. Sample 185-1149B-20R-1, 55–57 cm, yields in association *Mirifusus dianae minor* Baumgartner, *Homeoparonaella peteri* Jud, *S.*? *tripes* Jud, *Sethocapsa leiostraca* Foreman, *Obesacapsula verbana* (Parona), and *Svinitzium columnarium* Jud (Fig. F3).

Samples 185-1149B-19R-1, 23–25 cm; 18R-1, 109–112 cm; 18R-1, 29–32 cm; 17R-1, 0–4 cm; 16R-CC, 0–5 cm; and 16R-1, 3–5 cm, are assigned to UAZ 95 20 (Fig. F3), which was correlated to the interval M8–M4 (middle–late Hauterivian) (Fig. F2) (Jud, 1994; Baumgartner et al., 1995b).

In Samples 185-1149B-16R-CC, 0–5 cm, and 16R-1, 3–5 cm, corresponding to the top of the calcareous Unit IV, *Aurisaturnalis carinatus carinatus* (Foreman) is present. Dumitrica and Dumitrica-Jud (1995) showed that *Aurisaturnalis carinatus* represents a remarkable example of phyletic gradualism of an anagenetic type. *A. carinatus* is a highly polytypical species consisting of several successive morphotypes that may systematically represent a similar number of allochrone subspecies with high biostratigraphic value for the Hauterivian–Barremian interval. The authors have correlated the presence of the morphotypes with magnetic chrons. The first occurrence of *A. carinatus carinatus* was correlated with the uppermost M4 (uppermost Hauterivian or lowermost Barremian). The presence of *A. carinatus carinatus* in the Samples 185-1149B-16R-CC, 0–5 cm, and 16-R1, 3–5 cm, can precisely determine, therefore, the age attribution of the top of calcareous unit to the latest Hauterivian–earliest Barremien (magnetic Chron M4).

Unit III

Sample 185-1149B-15R-1, 0–3 cm, located at the base of the biosiliceous Unit III, is assignable to the Asseni–lower part of Verbeeki Zones (UA 1–3; Barremian–early Aptian) of O'Dogherty (1994), or to the UAZ 95 21–22 (Fig. F2). The radiolarian association of *Stichomitra communis* Squinabol and *Pseudodictyomitra carpatica* (Lozyniak) attributes Sample 185-1149B-13R-1, 0–6 cm, to the Verbeeki Zone of O'Dogherty (1994) (UA 5; early Aptian). Sample 185-1149B-4R-1, 25–28 cm, located at the top of the biosiliceous unit, is characterized by the concurrent presence of *Acanthocircus levis* (Donofrio and Mostler) and *Sciadiocapsa speciosa* (Squinabol), and it is assignable to the Romanus–Missilis Zones of O'Dogherty (1994) (UA 11–12; middle Albian).

CARBON ISOTOPE STRATIGRAPHY

All stable isotopic analyses were carried on bulk rock samples (nannofossil chalk/marl). Rock powder samples were analyzed for carbon isotopic composition at the Laboratory of Isotope Geochemistry at the University of Lausanne. Samples were measured for their carbonate $\delta^{13}C$ content, following the standard procedure of McCrea (1950), reacted at 50°C for one-half hour. A fractionation factor of 1.00931 between $CaCO_3$ and H_3PO_4 was applied (Swart et al., 1991). Carbonate $\delta^{13}C$ values were measured in a Finningan Mat Δ-S mass spectrometer. All $\delta^{13}C$ values are reported relative to the Peedee belmnite standard (*Belemnitella americana;* Peedee Formation, Cretaceous, South Carolina). The standard deviation of the analyses is ±0.05‰ for $\delta^{13}C$.

The $\delta^{13}C$ values are stable at ~1.75‰ from Samples 185-1149B-29R-1, 67–68 cm, through 24R-1, 21–24 cm, then sharply increase to a peak (3‰–3.5‰) in Samples 23R-1, 22–26 cm; 22R-1, 64–65 cm; and 22R-1, 17–20 cm, corresponding to radiolarian UAZ 95 18 (late Valanginian) (Fig. F2). From Samples 185-1149B-20R-1, CC through 16R-1, 92–96 cm (UAZ 95; 19–UAZ 95 20; Hauterivian), the values gradually decrease to ~2.5‰ (Fig. F2).

Several workers demonstrated the excellent reproducibility of the upper Valanginian positive carbon isotope excursion almost in Tethyan and Atlantic domains (e.g., Lini et al., 1992; Wortmann and Weissert, 2001). In Tethyan land sections, this excursion was correlated with magneto, ammonite, calcareous nannofossil, and radiolarian stratigraphy (Lini et al., 1992; Channell et al., 1993; Jud, 1994; Henning et al., 1999). The shape of the Valanginian $\delta^{13}C$ curve is, therefore, a powerful tool for indirect correlation with magnetic chrons. The rapid transition of C isotope ratios to positive values (see the interval from Cores 185-1149B-23R to 22R) (Fig. F2) can be correlated to the top of magnetic Chron M12 and the base of magnetic Chron M11 (Channell et al., 1993). The maximum values of $\delta^{13}C$ at Core 185-1149B-22R (Fig. F2) are indirectly correlatable to Chron M11. In Hole 1149B, probably because of discontinuous recovery, a double peak described in Henning et al. (1999) has not been identified. The end of the C isotope excursion is dated in the southern Alps as M10N (Channell et al., 1993).

RADIOLARIAN COMPOSITION AND GEOCHEMICAL DATA

Comparing only well-preserved samples, the most remarkable variation in the faunal composition is peaks in abundance of *Pantanellium* in Cores 185-1149B-22R (UAZ 18) and 16R (UAZ 20). In Core 185-1149B-22R, maximal values of $\delta^{13}C$ were recorded. Core 185-1149B-16R represents the uppermost part of the calcareous unit and the transition with the siliceous unit. These peaks in abundance of *Pantanellium* in Cores 185-1149B-22R and 16R are also correlatable to maximal values in barium recorded in the sediments (Plank, Ludden, Escutia, et al., 2000).

DISCUSSION AND CONCLUSIONS

Site 1149 is located on a positive magnetic anomaly (Plank, Ludden, Escutia, et al., 2000). Two alternative models of the oceanic magnetic lineations of this part of the Pacific plate were supposed, one identifying the positive anomaly at Site 1149 as Chron M12 and the other as Chron M11 (Plank, Ludden, Escutia et al., 2000; Nakanishi et al., 1992). In Hole 1149B, a sharp $\delta^{13}C$ positive peak (3‰–3.5‰) was identified in Cores 185-1149B-23R and 22R, and it was dated as late Valanginian by means of the radiolarian UAZ 95 18 (Fig. F2). In the Tethyan land sections, UAZ 95 18 is also coincident with maximum values of $\delta^{13}C$ (Jud, 1994; Baumgartner et al., 1995b). The upper Valanginian positive peak was correlated to Chron M11 (Channel et al., 1993) (Fig. F2). Because at Site 1149 the upper Valanginian $\delta^{13}C$ positive peak is situated in Cores 185-1149B-23R and 22R (Fig. F2), the magnetostratigraphic correlation of the basement with Chron M11 can be excluded. In Hole 1149D, at the direct contact with basalt, a radiolarian assemblage assignable to UAZ 95 16 was recovered. In the Tethyan land sections, the UAZ 95 16 was correlated with magnetic polarity zone interval M14 to M12. The radiolarian data together with the shape of $\delta^{13}C$ curve (Fig. F2) strongly supports, therefore, the magnetostratigraphic correlation of Site 1149 with Chron M12.

The upper Valanginian $\delta^{13}C$ positive peak recorded in Hole 1149B is coincident with high concentrations of barium in sediments and high abundances of *Pantanellium* in radiolarian assemblages. Barium is an indicator of high biogenic input (Lea and Boyle, 1990; Von Breymann et al., 1992; Klump et al., 2000). The observed positive correlation between abundance of *Pantanellium* and barium proves that certain paleoecological effects are highly influencing the faunal assemblages and that *Pantanellium* can be considered as a marker of high primary productivity conditions. The Pantanellids were mentioned as indicators of upwelling conditions by Baumgartner (1987). High abundances of the taxa *Pantanellium squinaboli squinaboli* have also been observed in Zones E2 and F1 from the Bosso section (central Italy) by Jud (1994). Zones E2 and F1 (Jud, 1994) correspond to UAZ 17 and 18 (Baumgartner et al., 1995b) and are correlatable with the upper Valanginian positive excursion.

The upper Valanginian carbon isotope event was very well documented as almost in the Tethyan and Atlantic domains. It was attributed to perturbation of the global carbon cycle and collapse of carbonate production in a scenario of intensified greenhouse conditions (Weissert and Lini, 1991; Weissert et al., 1998; Wortmann and

Weissert, 2000). In such a scenario, an acceleration of the water cycle may have provoked an increase of weathering on the continents and input of nutrients in the basins, inducing eutrophication and a crisis of carbonate production (Weissert et al., 1998). The data from Leg 185 show that the upper Valanginian carbon positive excursion seems to mirror eutrophic conditions also in the northwestern Pacific setting (distal during the Cretaceous from detrital input from continents). Such an "oceanic eutrophication" may be linked to extensive volcanism. The late Valanginian $\delta^{13}C$ positive excursion is confirmed as a global event, probably linked to high primary productivity.

ACKNOWLEDGMENTS

I thank the Ocean Drilling Program and its staff for their assistance during the cruise and the sampling at the Gulf Coast Repository in College Station. I would like to thank Jean Guex and Carlota Escutia for their suggestions on this manuscript. I am grateful to Peter Baumgartner, Elisabetta Erba, Francesca Lozar, and Roger Larson for interesting discussions. The reviews by Luis O'Dogherty and an unknown reviewer greatly help us to improve this work.

This research used samples and/or data provided by the Ocean Drilling Program (ODP). ODP is sponsored by the U.S. National Science Foundation (NSF) and participating countries under management of Joint Oceanographic Institutions (JOI), Inc. The Swiss National Science Foundation is acknowledged for providing travel funds and grant for this research (project 2100-55573.98 to P.O. Baumgartner).

REFERENCES

Abrams, L.J., Larson, R.L., Shipley, T.H., and Lancelot, Y., 1992. The seismic stratigraphy and sedimentary history of the East Mariana and Pigafetta basins of the western Pacific. *In* Larson, R.L., Lancelot, Y., et al., *Proc. ODP, Sci. Results,* 129: College Station, TX (Ocean Drilling Program), 551–569.

Baumgartner, P.O., 1987. Age and genesis of Tethyan Jurassic radiolarites. *Eclogae Geol. Helv.,* 80:831–879.

Baumgartner, P.O., Bartolini, A., Carter, E.S., Conti, M., Cortese, G., Danelian, T., De Wever, P., Dumitrica, P., Dumitrica-Jud, R., Gorican, S., Guex, J., Hull, D.M., Kito, N., Marcucci, M., Matsuoka, A., Murchey, B., O'Dogherty, L., Savary, J., Vishnevskaya, V., Widz, D., and Yao, A., 1995a. Middle Jurassic to Early Cretaceous radiolarian biochronology of Tethys based on Unitary Associations, middle Jurassic to Lower Cretaceous radiolaria of Tethys: occurrences, systematics, biochronology. *In* Baumgartner, P.O., O'Dogherty, L., Gorican, S., Urquhart, E., Pillevuit, A., and De Wever, P. (Eds.), *Middle Jurassic to Lower Cretaceous Radiolaria of Tethys: Occurrences, Systematics, Biochronology.* Mem. Geol. (Lausanne), 23:1013–1048.

Baumgartner, P.O., O'Dogherty, L., Gorican, S., Dumitrica-Jud, R., Dumitrica, P., Pillevuit, A., Urquart, E., Matsuoka, A., Danelian, T., Bartolini, A., Carter, E.S., De Wever, P., Kito, N., Marcucci, M., and Steiger, T., 1995b. Radiolarian catalogue and systematics of middle Jurassic to Early Cretaceous Tethyan genera and species. *In* Baumgartner, P.O., O'Dogherty, L., Gorican, S., Urquhart E., Pillevuit, A., and De Wever, P. (Eds.), *Middle Jurassic to Lower Cretaceous Radiolaria of Tethys: Occurrences, Systematics, Biochronology.* Mem. Geol. (Lausanne), 23:37–685.

Channell, J.E.T., Erba, E., and Lini, A., 1993. Magnetostratigraphic calibration of the late Valenginian carbon isotope event in pelagic limestones from northern Italy and Switzerland. *Earth Planet. Sci. Lett.,* 118:145–166.

Dumitrica, P., 1997. On the status of the Lower Cretaceous radiolarian species *Alievium helene* Schaaf and of other related species. *Rev. Micropaleontol.,* 40:211–226.

Dumitrica, P., and Dumitrica-Jud, R., 1995. *Aurisaturnalis carinatus* (Foreman), an example of phyletic gradualism among saturnalid-type radiolarians. *Rev. Micropaleontol.,* 38:195–216.

Dumitrica, P., Immenhauser, A., and Dumitrica-Jud, R., 1997. Mesozoic radiolarian biostratigraphy from Masirah Ophiolite, Sultane of Oman. Part I: middle Triassic, uppermost Jurassic and lower Cretaceous Spumellarians and multisegmented Nassellarians. *Bull. Nat. Mus. Natur. Sci.,* 9:1–106.

Guex, J., 1991. *Biochronological Correlations:* Berlin (Springer-Verlag).

Henning, S., Weissert, H., and Bulot, L., 1999. C-isotope stratigraphy, a calibration tool between ammonite- and magnetostratigraphy: the Valanginian–Hauterivian transition. *Geol. Carpathica,* 50:91–96.

Jud, R., 1994. Biochronology and systematics of Early Cretaceous radiolaria of the western Tethys. *Mem. Geol. (Lausanne),* 19:1–147.

Klump, J., Hebbeln, D., and Wefer, G., 2000. The impact of sediment provenance on barium-based productivity estimates. *Mar. Geol.,* 169:259–271.

Lea, D.W., and Boyle, E.A., 1990. A 210,000-year record of barium variability in the deep northwest Atlantic Ocean. *Nature,* 347:269–272.

Lini, A., Weissert, H., and Erba, E., 1992. The Valanginian carbon isotope event: a first episode of greenhouse climate conditions during the Cretaceous. *Terra Nova,* 4:374–384.

McCrea, J.M., 1950. On the isotopic chemistry of carbonates and a paleotemperature scale. *J. Chem. Phys.,* 18:849–857.

Nakanishi, M., Tamaki, K., and Kobayashi, K., 1992. Magnetic anomaly lineations from Late Jurassic to Early Cretaceous in the west-central Pacific Ocean. *Geophys. J. Int.,* 109:701–719.

O'Dogherty, L., 1994. Biochronology and paleontology of middle Cretaceous radiolarians from Umbria-Marche Appennines (Italy) and Betic Cordillera (Spain). *Mem. Geol. (Lausanne),* 21:1–351.

Plank, T., Ludden, J.N., Escutia, C., et al., 2000. *Proc. ODP, Init. Repts.,* 185 [CD-ROM]. Available from: Ocean Drilling Program, Texas A&M University, College Station TX 77845-9547, USA.

Savary, J., and Guex, J., 1999. Discrete biochronological scales and unitary associations: description of the BioGraph computer program. *Mem. Geol. (Lausanne),* 34:1–282.

Swart, P.K., Burns, S.J., and Leder, J.J., 1991. Fractionation of the stable isotopes of O and C in CO_2 during the reaction of calcite with phosphoric acid as a function of temperature and technique. *Chem. Geol.,* 86:89–96.

Von Breymann, M.T., Emeis, K.C., and Suess, E., 1992. Water depth and diagenetic constraints on the use of barium as a paleoproductivity indicator. *In* Summerhayes, C.P., Prell, W.L., and Emeis, K.C. (Eds.), *Upwelling Systems: Evolution Since the Early Miocene*. Spec. Publ.—Geol. Soc. London, 64:273–384.

Weissert, H., and Lini, A., 1991. Ice age interludes during the time of Cretaceous greenhouse climate? *In* Müller, D.W., McKenzie, J.A., and Weissert, H. (Eds.), *Controversies in Modern Geology: Evolution of Geological Theories in Sedimentology, Earth History and Tectonics:* New York (Academic Press), 173–191.

Weissert, H., Lini, A., Föllmi, K.B., and Kuhn, O., 1998. Correlation of Early Cretaceous carbon isotope stratigraphy and platform drowning events: a possible link? *Palaeogeogr., Palaeoclimatol., Palaeoecol.,* 137:189–203.

Wortmann, U.G., and Weissert, H., 2001. Tying platform drowning to perturbations of the global carbon cycle with a $\delta^{13}C_{org}$-curve from the Valanginian of DSDP Site 416. *Terra Nova,* 12:289–294.

APPENDIX

Species List

Acaeniotyle dentata Baumgartner.
Acaeniotyle dentata Baumgartner, Baumgartner et al., 1995a, p. 49, pl. 3281, figs. 1–7; MRD (species code in mesozoic radiolarian data base published by Baumgartner et al., 1995a) 3281.

***Acaeniotyle diaphorogona* group** Foreman sensu Baumgartner
Acaeniotyle diaphorogona gr. Foreman sensu Baumgartner, Baumgartner et al., 1995a, p. 51, pl. 3090, figs. 1–6; MRD 3090.

Acaeniotyle (?) ***florea*** Ozvoldova
Acaeniotyle (?) *florea* Ozvoldova, Baumgartner et al., 1995a, p. 52, pl. 5032, figs. 1–6; MRD 5032.

Acaeniotyle (?) ***glebulosa*** (Foreman)
Acaeniotyle (?) *glebulosa* (Foreman), Baumgartner et al., 1995a, p. 52, pl. 5033, figs. 1–4; MRD 5033.

Acaeniotyle umbilicata (Rüst)
Acaeniotyle umbilicata (Rüst), Baumgartner et al., 1995a, p. 54, pl. 3092, figs. 1–8; MRD 3092.

Acanthocircus levis (Donofrio & Mostler)
Acanthocircus levis (Donofrio & Mostler), O'Dogherty, 1994, p. 251, 252, pl. 43, figs. 5–7.

Alievium regulare (Wu & Li)
Alievium helenae Schaaf, Baumgartner et al., 1995a, p. 80, pl. 3228, figs. 1, 3, 4; MRD 3228.
Alievium regulare (Wu & Li), Dumitrica, 1997, pl. 2, figs. 12–14; pl. 3, figs. 1–3, 5.

Angulobracchia (?) ***portmanni portmanni*** Baumgartner
Angulobracchia (?) *portmanni portmanni* Baumgartner, Baumgartner et al., 1995a, p. 90, pl. 3285, figs. 1–4; MRD 3285.

Archaeodictyomitra excellens (Tan)
Archaeodictyomitra excellens (Tan), Baumgartner et al., 1995a, p. 102, pl. 3287, figs. 1–7; MRD 3287.

Archaeodictyomitra (?) ***lacrimula*** (Foreman)
Archaeodictyomitra (?) *lacrimula* (Foreman), Baumgartner et al., 1995a, p. 102, pl. 5595, figs. 1–4; MRD 5595.

Archaeodictyomitra leptocostata (Wu & Li)
Dictyomitra pseudoscalaris (Tan) sensu Schaaf, Baumgartner et al., 1995a, p. 186, pl. 5927, figs. 1–3; MRD 5927.
Archaeodictyomitra leptocostata (Wu & Li), Dumitrica et al., 1997, p. 139, pl. 7, fig. 4.

Aurisaturnalis carinatus carinatus (Foreman)
Acanthocircus carinatus Foreman, Baumgartner et al., 1995a, p. 62, pl. 5012, figs. 2, 4, 5; MRD 5012.
Aurisaturnalis carinatus carinatus (Foreman), Dumitrica and Dumitrica-Jud, 1995, p. 212, pl. 2, figs. 1–7, 8–11; pl. 3, figs. 1–4, 6–9, 11–14.

Cecrops septemporatus (Parona)
Cecrops septemporatus (Parona), Baumgartner et al., 1995a, p. 138, pl. 5229, figs. 1–5; MRD 5229.
Crolanium spp.
Crolanium spp., Baumgartner et al., 1995a, p. 148, 149, pl. 6123, figs. 1–3; MRD 6123.

Crucella bossoensis Jud
Crucella bossoensis Jud, Baumgartner et al., 1995a, p. 150, pl. 5204, figs. 1–3; MRD 5204.

Crucella lipmanae Jud
Crucella lipmanae Jud, Baumgartner et al., 1995a, p. 156, pl. 5628, figs. 1, 2; MRD 5628.

Cyclastrum (?) ***luminosum*** Jud
Cyclastrum (?) *luminosum* Jud, Baumgartner et al., 1995a, p. 162, pl. 5266, figs. 1–4; MRD 5266.

Dactyliodiscus lenticulatus (Jud)
Godia lenticulata Jud, Baumgartner et al., 1995a, p. 228, pl. 5287, figs. 1–3; MRD 5287.
Dactyliodiscus lenticulatus (Jud), Dumitrica et al., 1997, p. 24, pl. 2, fig. 14.

Deviatus diamphidius (Foreman)
Deviatus diamphidius s.l. (Foreman), Baumgartner et al., 1995a, p. 172, pl. 3112, figs. 1–6; MRD 4073.

Dibolachras tytthopora Foreman
Dibolachras tytthopora Foreman, Baumgartner et al., 1995a, p. 180, pl. 5422, figs. 1–4; MRD 5422.

Dicerosaturnalis dicranacanthos (Squinabol)
Acanthocircus trizonalis dicranacanthos (Squinabol), emend. Foreman, Baumgartner et al., 1995a, p. 72, pl. 3087, figs. 1–8; MRD 3087.
Dicerosaturnalis dicranacanthos (Squinabol), Dumitrica et al., 1997, p. 18, pl. 1, fig. 15.

Emiluvia chica s.l. Foreman
Emiluvia chica s.l. Foreman, Baumgartner et al., 1995a, p. 198, pl. 3213, figs. 1–3; MRD 3213.

Eucyrtis columbaria Renz
Eucyrtis columbaria Renz, Baumgartner et al., 1995a, p. 224, pl. 5620, figs. 1–9; MRD 5620.

Homoeoparonaella peteri Jud
Homoeoparonaella peteri Jud, Baumgartner et al., 1995a, p. 276, pl. 5267, figs. 1–4; MRD 5267.

Jacus (?) ***italicus*** Jud
Jacus (?) *italicus* Jud, Baumgartner et al., 1995a, p. 288, pl. 5371, figs. 1–3; MRD 5371.

Mirifusus apenninicus Jud
Mirifusus apenninicus Jud, Baumgartner et al., 1995a, p. 308, pl. 5716, figs. 1–5; MRD 5716.

Mirifusus chenodes (Renz)
Mirifusus chenodes (Renz), Baumgartner et al., 1995a, p. 310, pl. 3162, figs. 1–7; MRD 3162.

Mirifusus dianae minor Baumgartner
Mirifusus dianae minor Baumgartner, Baumgartner et al., 1995a, p. 314, pl. 3286, figs. 1–5; MRD 3286.

Mirifusus odoghertyi Jud
Mirifusus odoghertyi Jud, Baumgartner et al., 1995a, p. 320, pl. 5721, figs. 1–4; MRD 5721.

Mirifusus petzholdti (Rüst)
Mirifusus petzholdti (Rüst), Baumgartner et al., 1995a, p. 320, pl. 5703, figs. 1–4; MRD 5703.

Obesacapsula rusconensis rusconensis Baumgartner
Obesacapsula rusconensis rusconensis Baumgartner, Baumgartner et al., 1995a, p. 348, pl. 3282, figs. 1–3; MRD 3282.

Obesacapsula verbana (Parona)
Obesacapsula verbana (Parona), Baumgartner et al., 1995a, p. 350, pl. 3202, figs. 1–8; MRD 3202.

Pantanellium* sp. aff. *P. cantuchapai Pessagno & MacLeod
Pantanellium sp. aff. *P. cantuchapai* Pessagno & MacLeod, Baumgartner et al., 1995a, p. 370, pl. 5065, figs. 1, 2; MRD 5065.

Pantanellium squinaboli (Tan)
Pantanellium squinaboli (Tan), Baumgartner et al., 1995a, p. 372, pl. 5607, figs. 1-7; MRD 5607.

Parvicingula (?) **sp. aff. *P. cincta*** (Hinde)
Parvicingula (?) sp. aff. *P. cincta* (Hinde), Baumgartner et al., 1995a, p. 404, pl. 5724, figs. 1, 2; MRD 5724.

Praexitus alievi (Foreman)
Xitus (?) alievi (Foreman), Baumgartner et al., 1995a, p. 636, pl. 5674, figs. 1–7; MRD 5674.
Praexitus alievi (Foreman), Dumitrica et al., 1997, p. 56, pl. 12, fig. 7.

Pseudodictyomitra carpatica (Lozyniak)
Pseudodictyomitra carpatica (Lozyniak), Baumgartner et al., 1995a, p. 446, 448, pl. 3293, figs. 1–7.

Pseudodictyomitra lanceloti Schaaf
Pseudodictyomitra lanceloti Schaaf, Baumgartner et al., 1995a, p. 448, pl. 5641, figs. 1–5; MRD 5641.

Pseudodictyomitra lilyae (Tan)
Pseudodictyomitra lilyae (Tan), Baumgartner et al., 1995a, p. 448, pl. 5641, figs. 1–5; MRD 5625.

Pseudocrolanium cristatum Jud
Pseudocrolanium cristatum Jud, Baumgartner et al., 1995a, p. 440, pl. 5521, figs. 1, 2; MRD 5521.

Pseudocrucella (?) ***elisabethae*** (Rüst)
Pseudocrucella (?) *elisabethae* (Rüst), Baumgartner et al., 1995a, p. 444, pl. 3947, figs. 1–4; MRD 3947.

Ristola asparagus Jud
Ristola asparagus Jud, Baumgartner et al., 1995a, p. 474, pl. 5575, figs. 1–6; MRD 5575.

Sciadiocapsa speciosa (Squinabol)
Sciadiocapsa speciosa (Squinabol), O'Dogherty 1994, p. 229, 230, pl. 38, figs. 11–20.

Sethocapsa dorysphaeroides Neviani sensu Schaaf
Sethocapsa dorysphaeroides Neviani sensu Schaaf, Baumgartner et al., 1995a, p. 494, pl. 5544, figs. 1–6; MRD 5544.

Sethocapsa* sp. aff. *S. kaminogoensis Aita
Sethocapsa sp. aff. *S. kaminogoensis* Aita, Baumgartner et al., 1995a, p. 496, pl. 5481, figs. 1–7; MRD 5481.

Sethocapsa leiostraca Foreman
Sethocapsa leiostraca Foreman, Baumgartner et al., 1995a, p. 498, pl. 3062, figs. 1–5; MRD 3062.

Sethocapsa (?) ***orca*** Foreman
Sethocapsa (?) *orca* Foreman, Baumgartner et al., 1995a, p. 498, pl. 5553, figs. 1–5; MRD 5553.

Sethocapsa simplex Taketani
Sethocapsa simplex Taketani, Baumgartner et al., 1995a, p. 500, pl. 5469, figs. 1–3; MRD 5469.

Sethocapsa trachyostraca Foreman
Sethocapsa trachyostraca Foreman, Baumgartner et al., 1995a, p. 500, pl. 5469, figs. 1–3; MRD 3063.

Sethocapsa tricornis Jud
Sethocapsa tricornis Jud, Baumgartner et al., 1995a, p. 502, pl. 5510, figs. 1–3; MRD 5510.

Sethocapsa uterculus (Parona) sensu Foreman
Sethocapsa uterculus (Parona) sensu Foreman, Baumgartner et al., 1995a, p. 504, pl. 5462, figs. 1–8; MRD 5462.

Spongocapsula* sp. aff. *S. coronata (Squinabol)
Spongocapsula sp. aff. *S. coronata* (Squinabol), Baumgartner et al., 1995a, p. 511, pl. 5773, fig. 1; MRD 5773.

Spongocapsula (?) ***tripes*** Jud
Spongocapsula (?) *tripes* Jud, Baumgartner et al., 1995a, p. 514, pl. 5526, figs. 1–6; MRD 5526.

Stichomitra communis Squinabol
Stichomitra communis Squinabol, O'Dogherty 1994, p. 144–146, pl. 17, figs. 6–16.

Stylosphaera (?) ***macroxiphus*** (Rüst)
Stylosphaera (?) *macroxiphus* (Rüst), Baumgartner et al., 1995a, p. 536, pl. 5044, figs. 1–5; MRD 5044.

Suna echiodes (Foreman)
Suna echiodes (Foreman), Baumgartner et al., 1995a, p. 540, pl. 3094, figs. 1–5; MRD 3094.

Suna hybum (Foreman)
Suna hybum (Foreman), Baumgartner et al., 1995a, p. 540, pl. 5049, figs. 1–5; MRD 5049.

Svinitzium columnarium Jud
Wrangellium (?) *columnarium* Jud, Jud, 1994, p. 116, pl. 23, figs. 14–16.
Wrangellium (?) *columnum* (Rüst), Baumgartner et al., 1995a, p. 630–631, pl. 5580, figs. 1–3; MRD 5580.
Svinitzium columnarium Jud, Dumitrica et al., 1997, p. 53, pl. 11, fig. 12.

Svinitzium pseudopuga Dumitrica
Wrangellium puga (Schaaf), Baumgartner et al., 1995a, p. 634, pl. 5636, figs. 1–6; MRD 5636.
Svinitzium pseudopuga Dumitrica, Dumitrica et al., 1997, p. 54, pl. 11, fig. 16.

Syringocapsa limatum Foreman
Syringocapsa limatum Foreman, Baumgartner et al., 1995a, p. 548, pl. 5426, figs. 1–5; MRD 5426.

Tethysetta usotanensis (Tumanda)
Parvicingula usotanensis Tumanda, Baumgartner et al., 1995a, p. 414, pl. 5712, figs. 1–6; MRD 5712.

Tethysetta usotanensis (Tumanda), Dumitrica et al., 1997, p. 51, pl. 10, fig. 14.

Thanarla elegantissima (Cita) sensu Sanfilippo & Riedel
Thanarla elegantissima (Cita) sensu Sanfilippo & Riedel, Baumgartner et al., 1995a, p. 566, pl. 5296, figs. 1–4; MRD 5296.

Thanarla gutta Jud
Thanarla gutta Jud, Baumgartner et al., 1995a, p. 568, pl. 5904, figs. 1–5; MRD 5904.

Thanarla pulchra (Squinabol) sensu Sanfilippo & Riedel
Thanarla pulchra (Squinabol) sensu Sanfilippo & Riedel, Baumgartner et al., 1995a, p. 570, pl. 5073, figs. 1–5; MRD 5073.

***Tritrabs ewingi* s.l.** (Pessagno)
Tritra bs ewingi s.l. (Pessagno), Baumgartner et al., 1995a, p. 606, pl. 3113, figs. 1–8; MRD 3113.

Xitus robustus Wu
Xitus sp. aff. *X. spicularius* (Aliev), Baumgartner et al., 1995a, p. 646, pl. 3295, figs. 1, 2, 4, 5.
Xitus robustus Wu, Dumitrica et al., 1997, p. 57, pl. 13, figs. 10, 11; MRD 3295.

Xitus vermiculatus (Renz)
Novixitus (?) *tuberculatus* (Wu), Baumgartner et al., 1995a, p. 338, pl. 5693, figs. 1–5; MRD 5693.
Xitus vermiculatus (Renz), Dumitrica et al., 1997, p. 57–58, pl. 12, figs. 5, 10.

Figure F1. Location of ODP Site 1149. OFZ = Ogasawara Fracture Zone, MSM = Magellan Seamount Flexural Moat, PB = Pigafetta Basin, EMB = east Mariana Basin, N. Smt. Prov. = northern Mariana Seamount Province (adaptation from figure 2 of Abrams et al. [1992], p. 553).

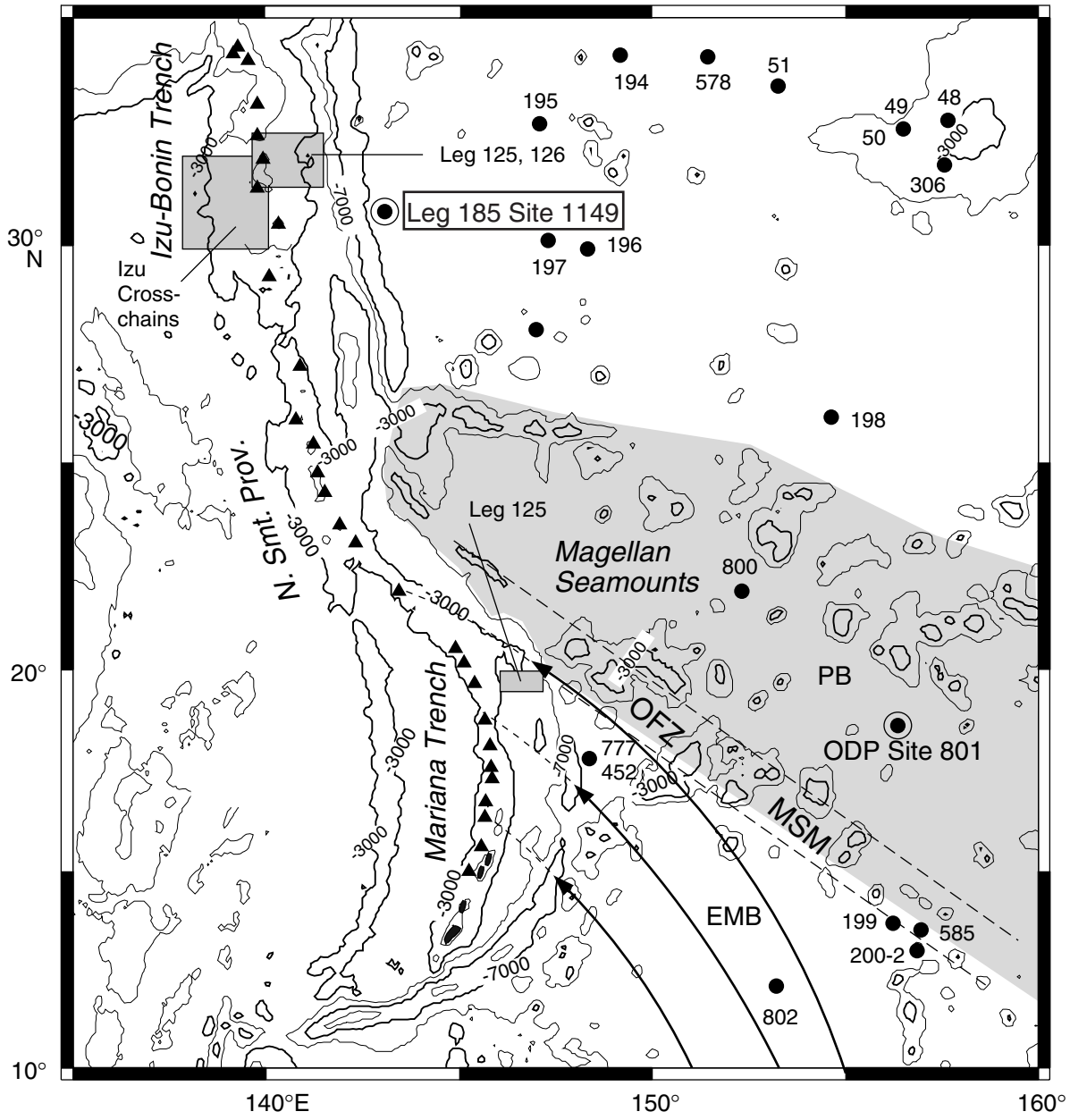

Figure F2. Summary of the lithostratigraphic section and radiolarian biochronology Unitary Association Zones (UAZs) of Units IV and III in Hole 1149B. Correlation of carbon isotope stratigraphy and radiolarian biochronology of Pacific Site 1149 with the Capriolo section (southern Alps, north Italy). In Tethyan sections, such as Capriolo, carbon isotope curves and radiolarian biochronology were well calibrated with polarity chrons (Lini et al., 1992; Channell et al., 1993; Jud, 1994). Thanks to the shape of $\delta^{13}C$ curve and radiolarian UAZ, the discontinuous recovered sedimentary section in Hole 1149B can, therefore, be indirectly correlated with polarity chrons. TD = total depth.

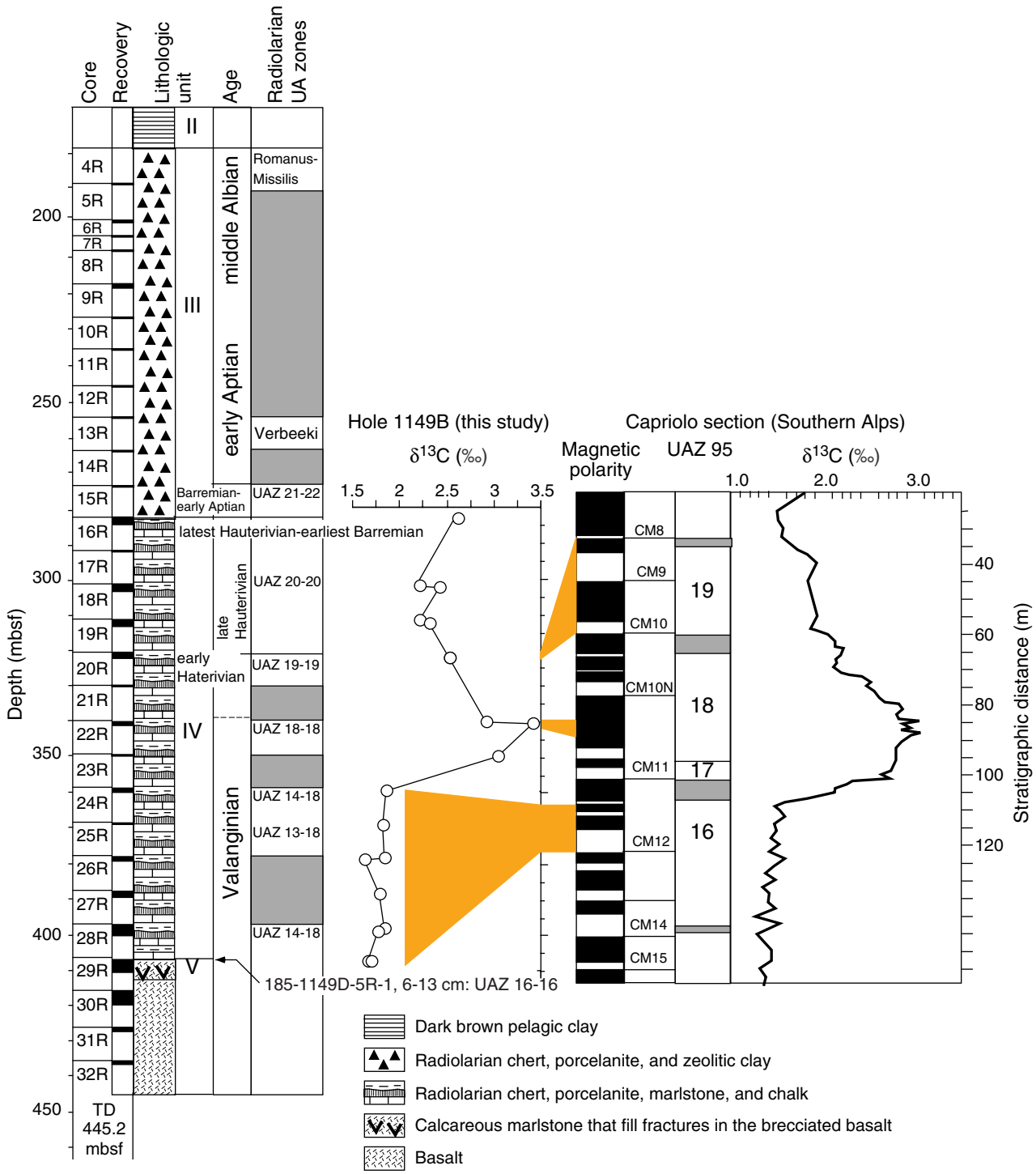

Figure F3. For the best preserved samples from Unit IV, the presence of treated radiolarian taxa is arranged in order of their first and last occurrence. At right, the resulting Unitary Association (UA) and Unitary Association Zone (UAZ) are indicated for each sample. UA refer to the 127 unitary associations that are the basis for the UAZ 95 (Baumgartner et al., 1995a). (**Figure shown on next page.**)

Figure F3 (continued). (Caption shown on previous page.)